HHS Public Access

Author manuscript

Transl Res. Author manuscript; available in PMC 2019 May 01.

Published in final edited form as:

Transl Res. 2018 May ; 195: 13–24. doi:10.1016/j.trsl.2017.12.001.

Intraoperative optical coherence tomography of the human thyroid: Feasibility for surgical assessment

Sarah J. Erickson-Bhatt[1,2,*], **Kelly J. Mesa**[1,3,*], **Marina Marjanovic**[1,4], **Eric J. Chaney**[1], **Adeel Ahmad**[1], **Pin-Chieh Huang**[1,4], **Z. George Liu**[5], **Kelly Cunningham**[5], and **Stephen A. Boppart**[1,3,4,5,6]

[1]Beckman Institute for Advanced Science and Technology, University of Illinois at Urbana-Champaign, Urbana, Illinois

[2]Morgridge Institute for Research, University of Wisconsin, Madison, Wisconsin

[3]Department of Electrical and Computer Engineering, University of Illinois at Urbana-Champaign, Urbana, Illinois

[4]Department of Bioengineering, University of Illinois at Urbana-Champaign, Urbana, Illinois

[5]Carle Foundation Hospital, Urbana, Illinois

[6]College of Medicine, University of Illinois at Urbana-Champaign, Urbana, Illinois

Abstract

Thyroid nodules assessed with ultrasound and fine needle aspiration biopsy are diagnosed as “suspicious” or “indeterminate” in 15–20% of the cases. Typically, total thyroidectomy is performed in such cases; however, only 25–50% are found to be cancerous upon final histopathologic analysis. Here we demonstrate optical coherence tomography (OCT) imaging of the human thyroid as a potential intraoperative imaging tool for providing tissue assessment in real-time during surgical procedures. Fresh excised tissue specimens from 28 patients undergoing thyroid surgery were imaged in the lab using a benchtop OCT system. Three-dimensional (3D) OCT images showed different microstructural features in normal, benign, and malignant thyroid tissues. A similar portable OCT system was then designed and constructed for use in the operating room, and intraoperative imaging of excised thyroid tissue from 6 patients was performed during the surgical procedure. The results demonstrate the potential of OCT to provide real-time imaging guidance during thyroid surgeries.

Corresponding Author: Stephen A. Boppart, M.D., Ph.D., Beckman Institute for Advanced Science and Technology, 405 N. Mathews Ave., Urbana, IL 61801, TEL (217) 244-7479, boppart@illinois.edu, Web http://biophotonics.illinois.edu.

*Authors contributed equally to the study.

Introduction

Thyroid cancer is the most common cancer of the endocrine system, and the National Cancer Institute predicted 56,870 new cases of thyroid cancer and 2,010 deaths in the U.S. in 2017.[1] The thyroid gland consists of two connected lobes located at the front of the neck which wrap around the trachea. The gland produces the hormones L-thyroxine (T4) and L-triiodothyronine (T3), which regulate metabolic physiological processes, cellular respiration, total energy expenditure, growth and maturation of tissues, and turnover of hormones, substrates, and vitamins. Parathyroid glands, located at the back of the thyroid, produce parathyroid hormone which, along with calcitonin, is involved in regulating the amount of calcium in the blood and bones.[2]

Following manual palpation of the neck as part of the physical exam, ultrasonography is often the first imaging modality employed to evaluate the presence of a thyroid nodule since it is readily accessible, inexpensive, noninvasive, and requires no radiation exposure. Ultrasound imaging is also effective at delineating intrathyroidal architecture, distinguishing cystic from solid lesions, determining if a nodule is solitary or part of a multinodular gland, and accurately locating and measuring the dimensions of a nodule. However, ultrasonography is dependent on an ultrasonographer for the quality of images, regions of the neck covered, and interpretation. Other less common methods include radionuclide imaging (RNI), positron emission tomography (PET), single photon emission computed tomography (SPECT), x-ray computed tomography (CT), and magnetic resonance imaging (MRI), but these clinical imaging modalities are usually insufficient to provide accurate diagnosis of malignant nodules. Therefore, fine needle aspiration biopsy (FNAB) is currently used as the gold standard for deciding whether to proceed with surgical treatment of thyroid nodules. FNAB results in four possible diagnoses: (1) benign nodule (occurs in ~70% of the cases, the recommended procedure is usually to follow the nodule without surgery); (2) malignant nodule (occurs in 4% of the cases, the recommended procedure is usually partial or total thyroidectomy); (3) suspicious nodule (occurs in 15–25% of the cases, the surgeon determines case-by-case how to proceed - typically total thyroidectomy or possibly lobectomy with frozen section analysis to determine malignancy); (4) non-diagnostic (which occurs in 5–10% of the cases when insufficient cytological material is present to make a diagnosis; the typical procedure is to repeat the FNAB or proceed with surgery).[2–4]

About 15–25% of thyroid nodule cases are found to be “cytologically indeterminate” and termed as follicular neoplasm, suspicious for carcinoma, or atypical.[5–7] This may be due to various benign cellular or nuclear changes which can be indistinguishable from papillary carcinoma, which can be metastatic. Additionally, features such as capsular penetration and vascular structures indicative of follicular carcinoma cannot be discerned in aspiration cytology due to disruption of the tissue architecture. The American Thyroid Association and the European Thyroid Association have recommended partial or total thyroidectomy in most indeterminate cases due to the possibility of carcinoma; however, only about 25–50% of the cases are found to be cancerous by post-surgical histological analysis. Hemi-thyroidectomy is preferred when possible due to lower morbidity,[8] and many patients will not require exogenous levothyroxine if half of the thyroid is functional.[6]

Optical coherence tomography (OCT) is the optical analogue to ultrasound imaging, but uses broadband near-infrared light to produce much higher resolution images with the tradeoff of reduced imaging depth penetration[9] (1). OCT has been widely used for clinical ophthalmic imaging[10] (2) and has demonstrated clinical translation in other areas as well including gastroenterology[11–12], dermatology[13–14], cardiology[15–16], and primary care[17]. OCT has also been used for cancer imaging and demonstrated the capability of imaging breast cancer intraoperatively[18–20] and *in vivo* within the surgical cavity[21] for real-time surgical guidance. OCT has demonstrated the ability to distinguish normal, benign, and malignant thyroid tissue on *ex vivo* specimens[22–23] as well as to identify thyroid and parathyroid glands on *ex vivo* specimens and intraoperatively.[24–25] However, none of these studies have demonstrated the ability to image *in vivo*. From benchtop to the operating room, this paper demonstrates the feasibility and potential of OCT as a tool for intraoperative surgical guidance during thyroid procedures.

Materials and Methods

Benchtop OCT system

The benchtop OCT system (Figure 1) consisted of a superluminescent diode source with 1,310 nm center wavelength and 170 nm bandwidth. A 50/50 fiber coupler was used to split the beam between the reference and sample arms. The axial and transverse resolutions of the system were 6 μm and 16 μm, respectively. The optical power at the sample was less than 10 mW. Reflected light was detected using a spectrometer in this spectral-domain OCT configuration. The tissue was placed in a dish and noncontact imaging was performed in the x-y lateral directions (using two computer-controlled galvanometer-scanning mirrors) as well as in the axial (z) direction to generate 3D image data, which was immediately displayed on the computer monitor.

Ex vivo imaging using the benchtop OCT system

The *ex vivo* human tissue studies were approved by the Institutional Review Boards at the University of Illinois at Urbana-Champaign (UIUC) and Carle Foundation Hospital, Urbana, Illinois, and written informed consent was provided by all subjects. More than 100 tissue samples from 28 patients undergoing partial, total, or completion thyroidectomy were imaged. During histological processing after surgery, small samples (~1–1.5 cm) of thyroid tissue were selected by the pathologist assistant from the visually normal and abnormal regions of the same thyroid and were placed in saline on ice. The samples were transported to the lab to be imaged using the benchtop OCT system within 12 hours. Following OCT imaging, the tissues were inked at the imaging location and processed and stained in house by the researchers with hematoxylin and eosin for correlation with OCT images. The histology slides were viewed independently by a board-certified pathologist at Carle Foundation Hospital to assess whether the slice corresponding to the OCT image contained malignant, benign, or normal thyroid tissue, as indicated on the final pathology report.

Intraoperative imaging using a portable OCT system

A portable custom-designed spectral-domain OCT system was designed and constructed to be easily maneuvered into the operating room and positioned close to the surgical field for

real-time imaging during surgical procedures. The intraoperative OCT system (Figure 2) also used a superluminescent diode source (Praevium Research, Inc.; 1,330 nm center wavelength, 105 nm bandwidth) and a 50/50 fiber coupler to split light between the sample arm (the handheld surgical probe) and the reference arm. The reflected light was detected by a spectrometer and the 2D OCT images (B-scans) were displayed in real time on the computer screen with both axial and transverse resolutions of approximately 9 μm, an image scan width of 8.8 mm, and a frame rate of 11.5 frames/s. The laser power on the tissue was less than 10 mW.

Procedure for intraoperative imaging of thyroid specimens

The intraoperative study was also approved by the Institutional Review Boards at UIUC and Carle Foundation Hospital and written informed consent was provided by all subjects. The portable OCT system was brought into the operating room, outside of the sterile field, during the surgeries. The probe was covered with two sterile and optically transparent plastic sheaths and placed in contact with the fresh tissue specimens during imaging. In each case, the surgeon resected the thyroid, palpated the specimen, and subsequently made an incision along the longest axis of the thyroid as shown in Figure 3, with the future histological section plane depicted in blue. The tissue was then immediately given to the researchers for imaging the samples in a sweeping pattern.

Real-time OCT frames were displayed on the monitor and saved for later postprocessing. The real-time images were viewed only by the researchers in this study and were not used by the surgeon for diagnostic or surgical guidance purposes. Typically 1 to 3 areas were imaged for each tissue sample, and the imaging time for each specimen was less than one minute. Due to the standard tissue histological sectioning protocols at Carle Foundation Hospital, OCT imaging was performed in planes orthogonal to the histological sectioning planes, as depicted in Figure 3. Typically, the OCT imaged area was identified by the application of surgical ink. However, during the intraoperative imaging portion of this study, this was not allowed. Thus, after OCT imaging, the sample was placed in preserving solution (formalin) and sent for histological processing. The pathologist received the entire specimens with the surgical incisions made in the operating room for OCT imaging. The pathologist subsequently incised the tissue along the same direction as the incision in the operating room and generated histological slides of these imaged areas. The remainder of each tissue specimen was grossly dissected and submitted for histological processing and evaluation, as per standard-of-care. Histology slides from the OCT imaged areas were digitized with a slide scanner (NanoZoomer 2.0 RS, Hamamatsu C10730), and correlations were made between the OCT images the corresponding histological sections.

Results

Ex vivo bench-top 3D OCT imaging of normal, benign, and malignant human thyroid tissue

OCT images from the bench-top system were collected from 28 patients undergoing partial, total, and completion thyroidectomy. Table 1 shows the distribution of patients by gender and age (note that only two patients were male, which is consistent with thyroid diseases being more prevalent in females). The table lists the pre-operative diagnosis (determined by

fine-need aspiration biopsy (FNAB)), the surgical procedure, and the final post-operative diagnosis (from histopathological analysis) for each patient. Out of 28 patients, 14 had a pre-operative diagnosis of a “suspicious” or indeterminate nodule. Of these 14 patients, 13 underwent total thyroidectomy (~93%), and only 5 of the 13 (~38%) were found to be malignant upon final histological analysis. This is consistent with the statistics from the American and European Thyroid Associations.[6]

Representative examples of OCT images of normal and benign thyroid tissue are shown in Figure 4. The apparent differences in size or area of tissue between histology and OCT is due to the loss of portions of tissue that occurred during sectioning of histology (performed in house by researchers). The upper panel in Figure 4 shows images from a patient with both regions of goiter and normal thyroid. The OCT image in Fig. 4B shows rounded outlines of thyroid follicles with relatively uniform size and distribution, whereas the region containing goiter (Fig. 4E) shows regions of higher tissue density and inhomogeneous scattering, large differences in the size of the follicles, and deformation of the tissue structure. Videos of the 3D OCT data set as the imaging plane passes through the normal and goiter regions of the thyroid tissue are shown in the supplementary data (videos S1 and S2). The corresponding histology images are shown in Figs. 4C and 4F, respectively. In the lower panel in Figure 4 are images of normal (Fig. 4H) and diseased (Fig. 4K) thyroid regions from a patient with follicular adenoma, and the corresponding histology images (Figs. 4I and 4L, respectively). The image of the follicular adenoma exhibits enlarged follicles, denser tissue, and higher scattering compared to the image of the normal region.

The representative OCT image of papillary thyroid carcinoma (Fig. 5E) shows increased scattering and the formation of a tumor capsule, compared to normal thyroid tissue (Fig. 5B). Videos of the OCT image data as the imaging plane passes through the normal and papillary carcinoma regions of the thyroid tissue are shown in the supplementary data (videos S3 and S4). In a case where papillary thyroid carcinoma was combined with Hashimoto’s thyroiditis (HT), there was no normal tissue found in the thyroid because all the tissue surrounding the cancer contained HT (Fig. 5K). Hashimoto’s thyroiditis is an autoimmune thyroid disease which leads to hypothyroidism. While the presence of HT alone does not warrant surgery, the association with papillary thyroid carcinoma does require surgical removal, although the correlation between these two thyroid pathologies is not entirely understood.[26]

These imaging results using the benchtop system revealed OCT images with different features of normal, benign, and malignant human thyroid tissues. The high percentage of total thyroidectomies that result in benign outcomes upon final histopathology demonstrates the limitation of current diagnostic methods (i.e. ultrasound and FNAB). Improvements in imaging technology, particularly during surgical procedures, have the potential to improve patient outcomes by reducing unnecessary thyroidectomies and enabling visualization of cancer metastasis to lymph nodes and other regions of the neck.

Intraoperative imaging of human thyroid tissue

Thyroid specimens from 6 patients (3 males and 3 females, ages 43–61) who were undergoing total thyroidectomy (5 patients) and right hemithyroidectomy (1 patient) were

imaged in the operating room using the handheld probe immediately following surgical resection. One thyroid specimen could not be imaged due to the frail cystic nature of the nodular tissue, which ruptured when the surgeon attempted to expose the inner tissue for OCT imaging. The specimen did not contain tangible tissue inside the walls of the cystic thyroid nodule. Table 2 provides a summary of the human subject cases, including the procedure, the final post-operative diagnosis, and the nodule dimensions and location (if applicable). The final histopathological diagnoses included papillary carcinoma, multinodular goiter, and hyperthyroidism.

Representative OCT images of thyroid specimens using our portable intraoperative OCT imaging system are shown in Figs. 6 and 7. It should be noted that the images from the intraoperative system are cross-sectional and depth-resolved, whereas the images from the benchtop system are *en face,* or acquired in a plane parallel to the tissue surface. The benchtop system was configured on a vibration-isolation optical table and housed in the laboratory while the portable, self-contained intraoperative system was transported to and into the operating room where it was calibrated and tested after the patient was sedated, and before imaging. The benchtop system utilized a stationary sample arm which collects a single 3D OCT image volume, whereas the portable system has a handheld probe that can be swept along the tissue to generate video-based cross-sectional images in real-time. For the current study, some of the intraoperative thyroid specimens that were imaged were of comparable size to the probe tip which did not allow for good video-based image sweeps. For these cases, single sectional images are shown. Furthermore, the intraoperative tissue specimens were not flat, and the OCT operator was not allowed to physically alter the tissue in any way to accommodate for imaging. The tissue also had to be imaged quickly, approximately 5 seconds per area, since it was not placed in a preserving solution prior to OCT imaging. Two OCT operators were required per imaging session, where the first OCT operator would hold the handheld probe and specimen while the second operator would control the image acquisition, record the specimen orientation, and digitally photograph the specimen.

Fig. 6 shows representative intraoperative OCT images, corresponding histology, and a photo of the gross thyroid tissue from a patient with papillary carcinoma. The OCT images reveal dense highly-scattering tissue and an absence of any normal follicular structure. Fig. 6B clearly shows a margin between normal and cancerous tissue. The right side of the image shows normal follicular structures with the transition to papillary carcinoma towards the left where the follicular structures are overcome by dense, highly scattering tissue. Fig. 7 shows a representative intraoperative OCT image, corresponding histology, and photo of the gross thyroid tissue from a patient with toxic multinodular goiter. In the OCT image, the follicles appear enlarged and are separated from each other with an overall non-uniform structure.

These images demonstrate real-time imaging of thyroid tissues during surgical procedures. The images were collected using a handheld probe that is capable of imaging *in vivo* for real-time surgical guidance in future thyroid surgeries, as has been previously demonstrated during wide local excision of breast cancer[21]. OCT imaging with our handheld probe can provide real-time feedback during the procedure rather than waiting for post-operative histopathological diagnosis, with the overall goal to improve patient morbidity.

Discussion

This study demonstrated the ability to differentiate normal, benign and malignant thyroid tissues from the bench to the bedside (operating room). A benchtop OCT system was used to image fresh excised thyroid tissues from 28 patients to establish an atlas of different thyroid diseases and what types of features would be expected during intraoperative imaging. A portable OCT system was subsequently developed to translate the technology to the operating room and used to perform a feasibility study to demonstrate the ability to distinguish normal from benign and malignant tissue in 6 thyroid surgeries, showing the potential of the system for surgical guidance. Real-time OCT imaging during thyroid surgeries could potentially reduce the morbidity associated with total thyroidectomies by enabling surgeons to remove only the diseased portions of the thyroid. This would greatly improve patient lives since more than 50% of cases where total thyroidectomy was performed due to a suspicious nodule are found to be benign upon final histopathology analysis. Current imaging methods used for thyroid diagnostics (e.g. ultrasound, FNAB) do not provide real-time feedback during thyroid surgeries. Other groups have also demonstrated OCT of the human thyroid and the capability of this technology for differentiating cancerous and noncancerous thyroid tissue. Our system has the further capability of performing *in vivo* imaging of the tissue prior to surgical excision as well as imaging of the cavity to detect the presence of any remaining cancer. This has been demonstrated during wide local excision surgery of the breast and future work will demonstrate *in vivo* imaging during thyroid surgeries.

There are many challenges encountered when translating a new imaging technology from the bench to clinical use. For these current studies, the instrumentation and optical components of a benchtop OCT system were minimized to fit onto a portable cart which could be easily maneuvered into the operating room. The benchtop system was used initially to identify and establish basic microstructural tissue features that would likely be encountered when using the intraoperative system, and was used initially because it was more robust than the portable handheld system, being more stationary, mounted on an optical table, and located in an isolated laboratory setting. It should be noted that some imaging quality and system performance can be reduced by the nature of the imaging system being transported around the hospital, as opposed to being secured to a stable optical table in the lab. The diagnostic performance of the intraoperative system was demonstrated in a previous study using the intraoperative system to image breast tumor margins, which yielded a sensitivity and specificity of 91.7% and 92.1%, respectively.[21] Ongoing studies to image additional thyroid cases intraoperatively are being performed, and the standard sensitivity/specificity analysis will be performed based on diagnoses by clinicians trained on reading the OCT images. Additionally, a foot pedal can be incorporated into the system so that a single user can initiate and stop the recording of data; thus, minimizing the number of people in the operating room.

Another challenge during intraoperative imaging was the restriction that the OCT imaging plane be orthogonal to the histological sectioning plane. This prevented direct correlation and precise feature-matching between the OCT and histology images for the intraoperative cases, whereas with the benchtop system the excised tissues could be inked after imaging,

and the histology planes could be clearly matched by the study investigators. This allowed a more direct correlation between OCT and histology. Future studies will be performed where multiple tissue samples will be imaged with the portable OCT system in the pathology lab to achieve more direct histological comparisons, and for assessing the diagnostic accuracy of the system. Additionally, imaging the thyroid intraoperatively (and potentially *in vivo* in future studies) is restricted to the exposed surface and near-surface regions of the tissue, since OCT has an imaging depth of 1–2 mm. For the cases presented here, the surgeon made an incision in the thyroid to allow for direct imaging of the area of interest. For future *in vivo* studies, the surgical protocol would be modified such that once the thyroid is exposed but still in place during the surgery, the surgeon would use the probe to image regions of interest to further indicate the presence and extent of cancer. The imaging feedback occurs in real time at near-video rate and would require additional time on the order of about 5–10 minutes depending on the surgeon and the case. The immediate anticipated clinical impact would be for patients who are recommended to undergo total thyroidectomy for a suspicious nodule. For these cases, our system could be used to better explore the thyroid *in situ* during the open surgery, and the surgeon could modify the procedure to a hemi-thyroidectomy or lobectomy where appropriate to improve patient morbidity.

The implementation of OCT needle probes with the portable intraoperative system could be used to image and identify tissue microstructure in deeper regions of the thyroid.[27–28] In future studies, the portable system presented here could also be used to perform *in vivo* imaging of the surgical cavity and any exposed loco-regional lymph nodes with the handheld probe, immediately following removal of the primary specimen. This system and method has been previously demonstrated for breast cancer surgery.[21] This intraoperative *in vivo* imaging system would enable immediate visualization of any residual tumor tissue during surgery, as well as evidence of any disease in other regions of the neck and lymph nodes.[29]

Conclusion

This feasibility study demonstrated the translation of optical coherence tomography (OCT) imaging of the human thyroid from the bench to the operating room using a portable intraoperative system with a handheld surgical imaging probe. Further improvements to the technology would enable the surgeon to assess the *in vivo* thyroid, including deep thyroid nodules, in real time during surgery, and possibly reduce the number of unnecessary total thyroidectomies due to “suspicious” diagnoses.

Supplementary Material

Refer to Web version on PubMed Central for supplementary material.

Acknowledgments

The authors thank Darold Spillman for his operations and information technology support for this research. They also thank Christine Canfield and the clinical research and surgical nursing staff at Carle Foundation Hospital for their contributions. This research was supported in part by grants from the National Institutes of Health (R01 CA213149 and R01 EB013723). Additional information can be found at http://biophotonics.illinois.edu. Author S. J. E-B. would like to acknowledge support from a Beckman Institute Postdoctoral Fellowship. Author K. J. M. was supported by the National Science Foundation Graduate Research Fellowship Program. All authors have read the journal’s authorship agreement and the manuscript has been reviewed by and approved by all named authors.

Stephen Boppart discloses being co-founder and Chief Medical Officer of Diagnostics Photonics, which is commercializing interferometric synthetic aperture microscopy for intraoperative image guidance. He also receives royalties from patents licensed by the Massachusetts Institute of Technology related to optical coherence tomography. All other authors declare no conflicts of interest. All authors have read the journal's authorship agreement.

References

1. NCI SEER stats thyroid cancer fact sheet. https://seer.cancer.gov/statfacts/html/thyro.html
2. Terris, DJ., Gourin, CG., editors. Thyroid and parathyroid diseases: medical and surgical management. Thieme Medical Publishers, Inc; New York, NY: 2009.
3. Niedziela M. Thyroid nodules. Best Pract Res Clin Endocrinol Metab. 2014 Mar; 28(2):245–77. DOI: 10.1016/j.beem.2013.08.007 [PubMed: 24629865]
4. Chaudhary V, Bano S. Imaging of the thyroid: Recent advances. Indian J Endocrinol Metab. 2012 May; 16(3):371–6. DOI: 10.4103/2230-8210.95674 [PubMed: 22629501]
5. Castro MR, Gharib H. Continuing controversies in the management of thyroid nodules. Ann Intern Med. 2005 Jun 7; 142(11):926–31. [PubMed: 15941700]
6. Alexander EK. Approach to the patient with a cytologically indeterminate thyroid nodule. J Clin Endocrinol Metab. 2008 Nov; 93(11):4175–82. DOI: 10.1210/jc.2008-1328 [PubMed: 18987277]
7. Dobrinja C, Trevisan G, Piscopello L, Fava M, Liguori G. Comparison between thyroidectomy and hemithyroidectomy in treatment of single thyroid nodules identified as indeterminate follicular lesions by fine-needle aspiration cytology. Ann Ital Chir. 2010 Nov-Dec;81(6):403–10. [PubMed: 21456476]
8. Gibelli B, Dionisio R, Ansarin M. Role of hemithyroidectomy in differentiated thyroid cancer. Curr Opin Otolaryngol Head Neck Surg. 2015 Apr; 23(2):99–106. DOI: 10.1097/MOO.0000000000000142 [PubMed: 25692624]
9. Huang D, Swanson EA, Lin CP, et al. Optical coherence tomography. Science. 1991 Nov 22; 254(5035):1178–81. [PubMed: 1957169]
10. Baumal CR. Clinical applications of optical coherence tomography. Curr Opin Ophthalmol. 1999 Jun; 10(3):182–8. [PubMed: 10537777]
11. Das A, Sivak MV Jr, Chak A, et al. High-resolution endoscopic imaging of the GI tract: a comparative study of optical coherence tomography versus high-frequency catheter probe EUS. Gastrointest Endosc. 2001 Aug; 54(2):219–224. [PubMed: 11474394]
12. Tsai TH, Fujimoto JG, Mashimo H. Endoscopic optical coherence tomography for clinical gastroenterology. Diagnostics (Basel). 2014 May 5; 4(2):57–93. DOI: 10.3390/diagnostics4020057 [PubMed: 26852678]
13. Cao T, Tey HL. High-definition optical coherence tomography - an aid to clinical practice and research in dermatology. J Dtsch Dermatol Ges. 2015 Sep; 13(9):886–90. DOI: 10.1111/ddg.12768 [PubMed: 26882379]
14. Gambichler T, Jaedicke V, Terras S. Optical coherence tomography in dermatology: technical and clinical aspects. Arch Dermatol Res. 2011 Sep; 303(7):457–73. DOI: 10.1007/s00403-011-1152-x [PubMed: 21647692]
15. Cruz Ferreira R, Pereira-da-Silva T, Patrício L, Bezerra H, Costa M. Coronary optical coherence tomography: A practical overview of current clinical applications. Rev Port Cardiol. 2016 Feb; 35(2):105–12. DOI: 10.1016/j.repc.2015.09.016 [PubMed: 26852303]
16. Yonetsu T, Bouma BE, Kato K, Fujimoto JG, Jang IK. Optical coherence tomography– 15 years in cardiology. Circ J. 2013; 77(8):1933–40. [PubMed: 23856651]
17. Shelton RL, Jung W, Sayegh SI, McCormick DT, Kim J, Boppart SA. Optical coherence tomography for advanced screening in the primary care office. J Biophotonics. 2014 Jul; 7(7):525–33. DOI: 10.1002/jbio.201200243 [PubMed: 23606343]
18. Nguyen FT, Zysk AM, Chaney EJ, et al. Intraoperative evaluation of breast tumor margins with optical coherence tomography. Cancer Res. 2009 Nov 15; 69(22):8790–6. DOI: 10.1158/0008-5472.CAN-08-4340 [PubMed: 19910294]

19. Allen WM, Chin L, Wijesinghe P, et al. Wide-field optical coherence micro-elastography for intraoperative assessment of human breast cancer margins. Biomed Opt Express. 2016 Sep 19; 7(10):4139–4153. [PubMed: 27867721]
20. Mesa KJ, Selmic LE, Pande P, et al. Intraoperative optical coherence tomography for soft tissue sarcoma differentiation and margin identification. Lasers Surg Med. 2017 Mar; 49(3):240–248. DOI: 10.1002/lsm.22633 [PubMed: 28319274]
21. Erickson-Bhatt SJ, Nolan RM, Shemonski ND, et al. Real-time imaging of the resection bed using a handheld probe to reduce incidence of microscopic positive margins in cancer surgery. Cancer Res. 2015 Sep 15; 75(18):3706–12. DOI: 10.1158/0008-5472.CAN-15-0464 [PubMed: 26374464]
22. Pantanowitz L, Hsiung PL, Ko TH, et al. High-resolution imaging of the thyroid gland using optical coherence tomography. Head Neck. 2004 May; 26(5):425–34. [PubMed: 15122659]
23. Zhou C, Wang Y, Aguirre AD, et al. *Ex vivo* imaging of human thyroid pathology using integrated optical coherence tomography and optical coherence microscopy. J Biomed Opt. 2010 Jan-Feb; 15(1):016001.doi: 10.1117/1.3306696 [PubMed: 20210448]
24. Ladurner R, Hallfeldt KK, Al Arabi N, Stepp H, Mueller S, Gallwas JK. Optical coherence tomography as a method to identify parathyroid glands. Lasers Surg Med. 2013 Dec; 45(10):654–9. DOI: 10.1002/lsm.22195 [PubMed: 24249200]
25. Sommerey S, Al Arabi N, Ladurner R, et al. Intraoperative optical coherence tomography imaging to identify parathyroid glands. Surg Endosc. 2015 Sep; 29(9):2698–704. DOI: 10.1007/s00464-014-3992-x [PubMed: 25475518]
26. Anand A, Singh KR, Kushwaha JK, Hussain N, Sonkar AA. Papillary thyroid cancer and Hashimoto's thyroiditis: An association less understood. Indian J Surg Oncol. 2014 Sep; 5(3):199–204. DOI: 10.1007/s13193-014-0325-4 [PubMed: 25419066]
27. Lorenser D, Yang X, Kirk RW, Quirk BC, McLaughlin RA, Sampson DD. Ultrathin side-viewing needle probe for optical coherence tomography. Opt Lett. 2011 Oct 1; 36(19):3894–6. DOI: 10.1364/OL.36.003894 [PubMed: 21964133]
28. Zysk AM, Nguyen FT, Chaney EJ, et al. Clinical feasibility of microscopically-guided breast needle biopsy using a fiber-optic probe with computer-aided detection. Technol Cancer Res Treat. 2009 Oct; 8(5):315–21. [PubMed: 19754207]
29. Nolan RM, Adie SG, Marjanovic M, et al. Intraoperative optical coherence tomography for assessing human lymph nodes for metastatic cancer. BMC Cancer. 2016 Feb 23.16:144.doi: 10.1186/s12885-016-2194-4 [PubMed: 26907742]

Brief Commentary

Background Knowledge

About 15–25% of thyroid nodule cases are found to be “cytologically indeterminate”. Partial or total thyroidectomy is recommended in most indeterminate cases due to the possibility of carcinoma; however, only about 25–50% of the cases are found to be cancerous by post-surgical histological analysis.

Translational Significance

Optical coherence tomography (OCT) has demonstrated the ability to distinguish normal, benign, and malignant thyroid tissue on *ex vivo* specimens. From benchtop to the operating room, this paper demonstrates the feasibility and potential of OCT as a tool for intraoperative surgical guidance during thyroid procedures, which can reduce patient morbidity.

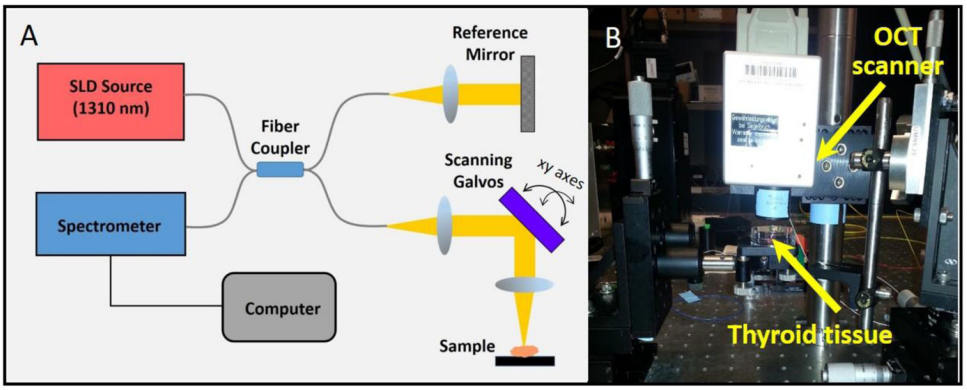

Fig. 1.

(A) Schematic of the benchtop OCT system. (B) Photograph of the system showing the position of the tissue during imaging.

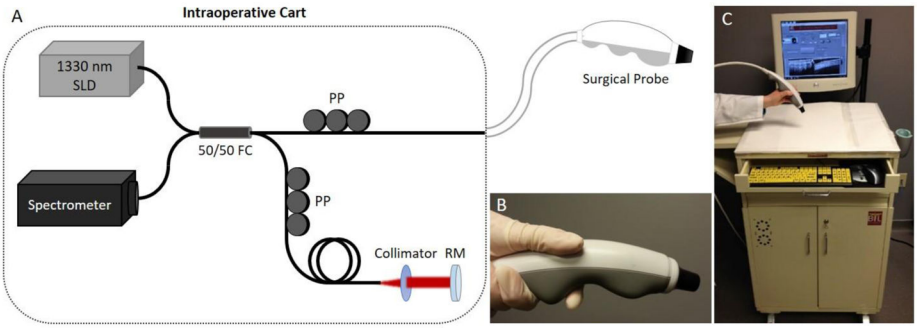

Fig. 2.

The intraoperative OCT imaging system. (A) Schematic showing the intraoperative OCT system components. (B) The sample arm is a handheld surgical probe used to image excised specimens. (C) The OCT system is integrated in a portable cart for easy transportation into the operating room and positioning near the sterile surgical field. SLD, superluminescent diode; FC, fiber optic coupler; PP, fiber polarization paddle controller; RM, reference mirror.

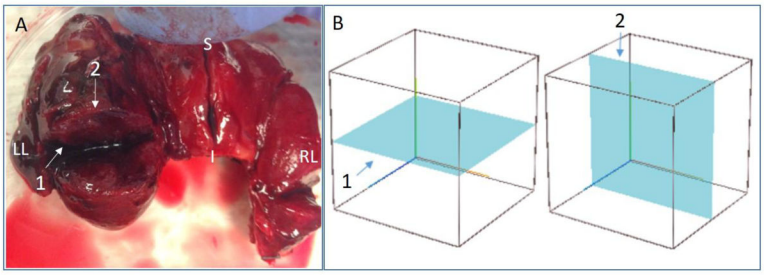

Fig. 3.

Histology and OCT imaging planes demonstrated on an excised thyroid with papillary carcinoma. (A) Thyroid tissue with three surgical incisions on right lobe, left lobe, and isthmus, respectively. (B) Schematic wire-frame block representing thyroid tissue along with the (1) OCT imaging plane and (2) orthogonal histological section plane.

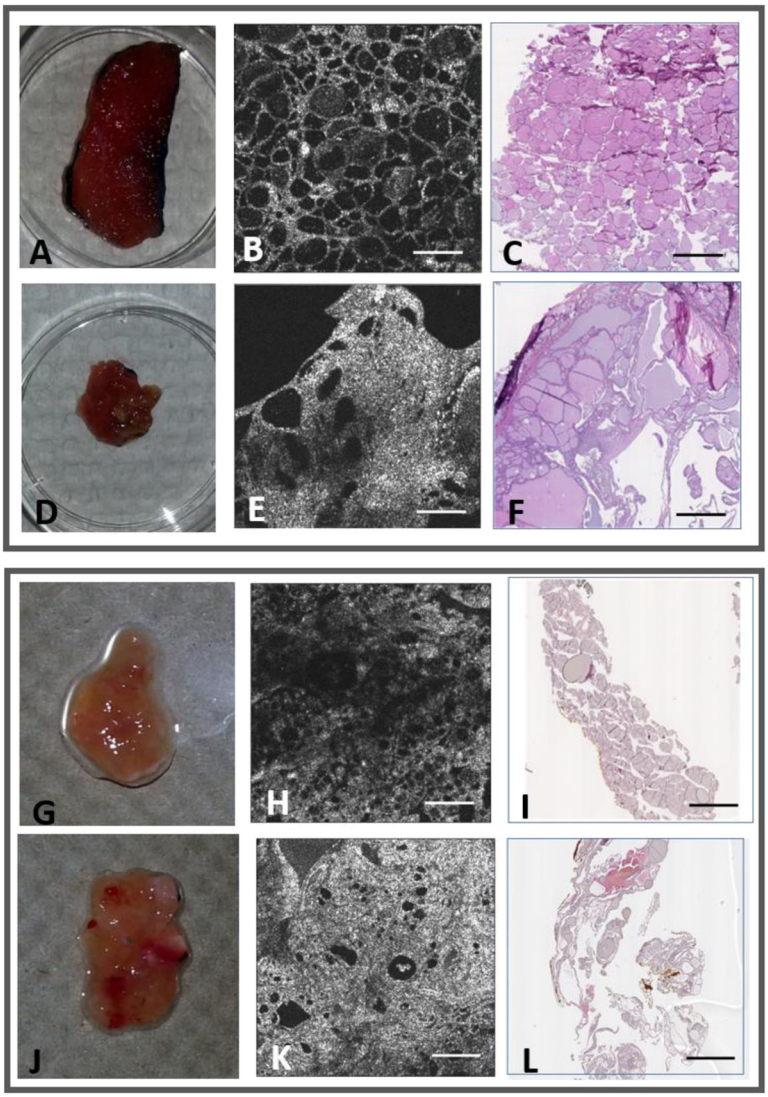

Fig. 4.

OCT and corresponding histology of normal and benign thyroid tissues. Upper Panel: (A, D) Photos and (B, E) OCT images of normal and goiter tissue regions from the same patient, along with (C, F) the corresponding histology images, respectively. Lower Panel: (G, J) Photos and (H, K) OCT images of normal and follicular adenoma tissue regions from the same patient, along with (I, L) the corresponding histology images, respectively. All scale bars: 1 mm.

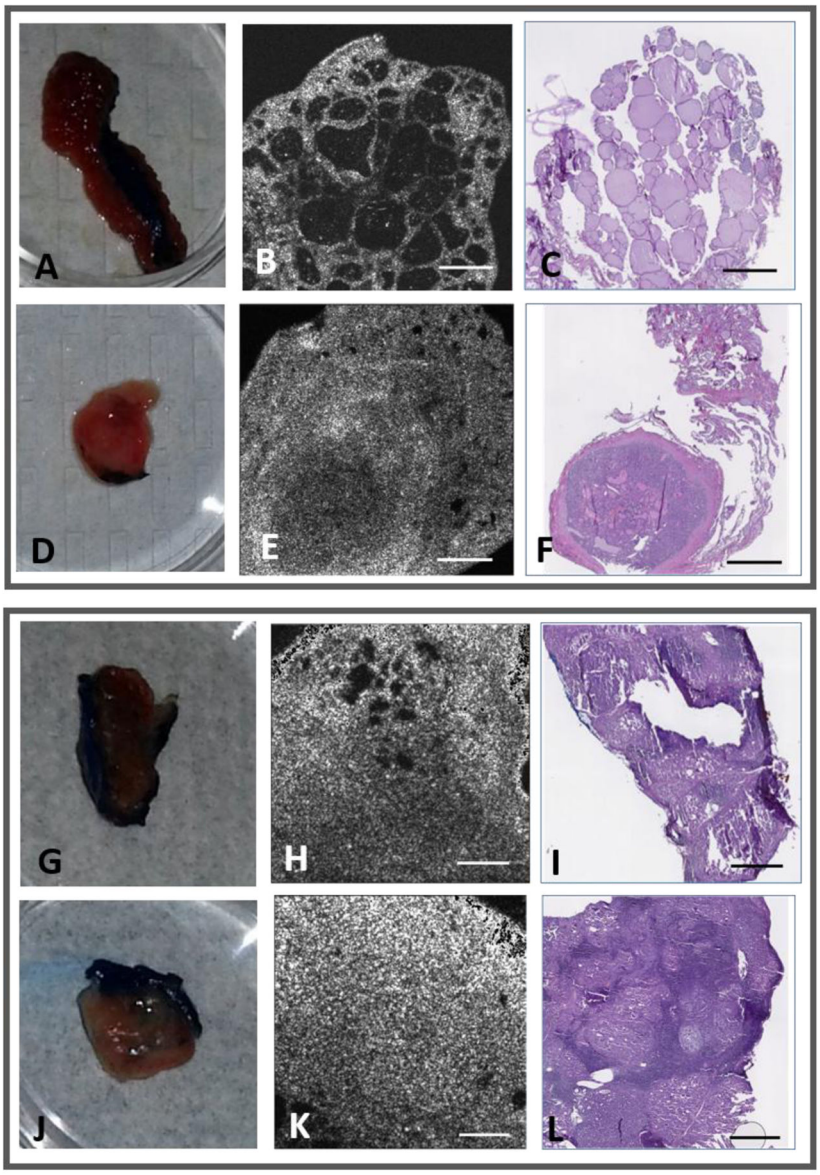

Fig. 5.

OCT and corresponding histology of normal, and papillary thyroid carcinoma tissues. Upper Panel: (A, D) Photos and (B, E) OCT images of normal and papillary thyroid carcinoma tissue regions from the same patient, along with (C, F) the corresponding histology images, respectively. Lower Panel: (G, J) Photos and (H, K) OCT images of Hashimoto's thyroiditis and papillary thyroid carcinoma tissue regions from the same patient, along with (I, L) the corresponding histology images, respectively. All scale bars: 1 mm.

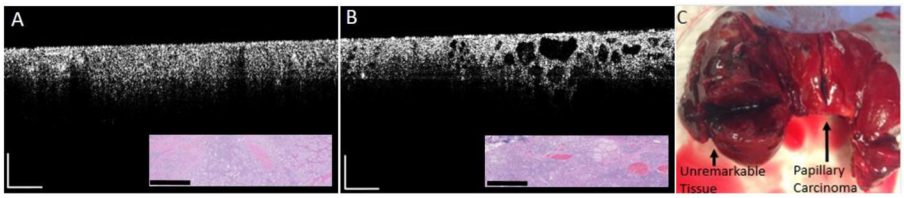

Fig. 6.

Intraoperative OCT images, corresponding histology, and a photo of the gross thyroid tissue from a patient with papillary carcinoma. (A) OCT image of papillary carcinoma with corresponding histology (inset). (B) OCT image of a margin that transitions from papillary carcinoma (left) to normal thyroid tissue (right) with corresponding histology (inset). (C) Total thyroidectomy specimen showing unremarkable left and right lobes as well as the isthmus with the localized papillary thyroid carcinoma. Scale bars represent 0.5 cm.

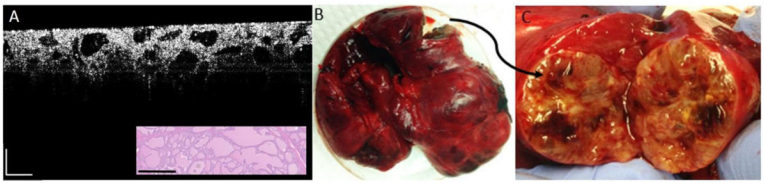

Fig. 7.

Intraoperative OCT image, corresponding histology, and photo of the gross thyroid tissue from a patient with toxic multinodular goiter. (A) OCT image with corresponding histology (inset). (B) Total thyroidectomy tissue confined in a Petri dish. (C) Photo of exposed tissue following surgical incision of the left lobe of thyroid tissue. Scale bars represent 0.5 cm.

Table 1

Summary of thyroid cases for tissues imaged ex vivo using the benchtop OCT system.

Gender	Age	Demographic	PreOp Diagnosis	Procedure	Final PostOp Diagnosis
F	--	--	suspicious thyroid nodule	total thyroidectomy	follicular adenoma
F	65	white, non-Hisp.	suspicious thyroid nodule	total thyroidectomy	follicular neoplasm
F	--	--	suspicious thyroid nodule	total thyroidectomy	nodular goiter
M	42	--	suspicious left thyroid nodule	total thyroidectomy	papillary microcarcinoma, follicular adenoma, multinodular goiter
F	35	white, non-Hisp.	multinodal goiter	completion thyroidectomy	multinodular colloid goiter
F	--	--	suspicious thyroid nodule	total thyroidectomy	multinodal goiter
F	24	--	papillary thyroid carcinoma	total thyroidectomy with right central neck dissection	papillary thyroid carcinoma, 12/16 positive nodes
F		white, non-Hisp.	suspicious thyroid nodule	total thyroidectomy	colloid goiter with focal adenomatous nodules.
F	31	white, non-Hisp.	Graves' disease	total thyroidectomy	papillary thyroid microcarcinoma two benign parathyroid glands (one intrathyroidal)
F	74	white, non-Hisp.	suspicious thyroid nodule	completion thyroidectomy	multinodular thyroid with adenomatous nodules, and focal Hurthle cell adenomatous nodule (left lobe)
F	64	white, non-Hisp.	papillary microcarcinoma	completion thyroidectomy	multinodular goiter and focal changes (papillary microcarcinoma).
F	--	--	suspicious thyroid nodule	total thyroidectomy	benign thyroid with diffuse hyperplasia
M	71	white, non-Hisp.	papillary carcinoma, right lobe.	total thyroidectomy	multinodular colloid goiter with Hurthle cell changes, lymphoid
F	66	--	multinodal goiter	total thyroidectomy	multinodular colloid goiter with post biopsy site changes
F	--	--	suspicious thyroid nodule	total thyroidectomy	papillary microcarcinoma, multinodular goiter
F	--	white, non-Hisp.	suspicious thyroid nodule	total thyroidectomy	goiter with hyperplastic changes, focal chronic inflammation, and focal entrapped parathyroid tissue; no malignancy is seen.
F	21	white, non-Hisp.	suspicious thyroid nodule	total thyroidectomy	benign thyroid with diffuse hyperplasia, goiter
F	28	white, non-Hisp.	left thyroid nodule	left hemithyroidectomy	nodular goiter with foci of chronic inflammation
F	65	non-Hisp., Afric. Amer.	toxic multinodular goiter	total thyroidectomy	toxic multinodular goiter
F	56	white, non-Hisp.	toxic multinodular goiter	total thyroidectomy	multinodular goiter with adenomatous follicular hyperplasia
F	66	--	multinodal goiter	total thyroidectomy	multinodular colloid goiter with dystrophic calcification
F	50	--	papillary thyroid carcinoma	total thyroidectomy	papillary carcinoma
F		white, non-Hisp.	suspicious thyroid nodule	total thyroidectomy	apillary carcinoma multiple benign colloid nodules and focal adenomatous hyperplasia.
F	26	--	suspicious thyroid nodule	total thyroidectomy	follicular carcinoma colloid goiter with adenomatous nodule

Gender	Age	Demographic	PreOp Diagnosis	Procedure	Final PostOp Diagnosis
F	69	--	Hurthle cell neoplasm	total thyroidectomy.	left thyroid nodule suspicious for Hurthle cell neoplasm
F	81	--	suspicious thyroid nodule	total thyroidectomy	papillary carcinoma, Hashimoto's thyroiditis.
F	46	--	papillary thyroid carcinoma	total thyroidectomy, limited central neck dissection	papillary carcinoma, follicular variant.0/6 lymph nodes
F	--	--	multinodular goiter/follicular neoplasm	total thyroidectomy	multiple follicular nodules; outside consultation pending

Table 2

Summary of thyroid cases imaged using the intraoperative OCT system.

Gender	Age	Procedure	Final Post Op Diagnosis	Nodule Dimension	Nodule Location	Other tissue
F	57	Total thyroidectomy	Multinodular goiter	3.0 mm largest dim.	Right lobe	Normal left lobe
M	53	Total thyroidectomy	Hyperthyroidism and nodule	(3.1 × 2.0 × 1.7) cm	Right lobe	Normal left lobe
F	43	Total thyroidectomy	Papillary carcinoma	(5.0 × 4.5 × 4.0) cm	Left and right lobe	N/A
F	59	Total thyroidectomy	Papillary carcinoma	(0.9 × 0.8 × 0.7) cm	Isthmus	Normal left and right lobe
M	59	Total thyroidectomy	Toxic multinodular goiter	2.5 cm largest dim.	Left lobe	N/A
M	61	Right hemithyroidectomy	Adenomatous nodule	Not applicable	N/A	parenchymal